

Amelogenesis imperfecta: A novel *FAM83H* mutation and characteristics of periodontal ligament cells

Nunthawan Nowwarote¹ | Thanakorn Theerapanon¹ | Thanaphum Osathanon² | Prasit Pavasant²  | Thanrira Porntaveetus¹  | Vorasuk Shotelersuk^{3,4}

¹Genomics and Precision Dentistry Research Unit, Department of Physiology, Faculty of Dentistry, Chulalongkorn University, Bangkok, Thailand

²Department of Anatomy, Faculty of Dentistry, Excellence Center in Regenerative Dentistry, Chulalongkorn University, Bangkok, Thailand

³Center of Excellence for Medical Genomics, Department of Pediatrics, Faculty of Medicine, Chulalongkorn University, Bangkok, Thailand

⁴Excellence Center for Medical Genetics, King Chulalongkorn Memorial Hospital, The Thai Red Cross Society, Bangkok, Thailand

Correspondence

Thanrira Porntaveetus, Department of Physiology, Faculty of Dentistry, Chulalongkorn University, Bangkok 10330, Thailand.
Email: thanrira.p@chula.ac.th

Funding information

Chulalongkorn Academic Advancement Into Its 2nd Century Project; Ratchadapisek Sompote Fund for Postdoctoral Fellowship, Chulalongkorn University; Thailand Research Fund (TRF), Grant/Award Number: DPG6180001; Office of Higher Education Commission (OHEC) Thailand, Grant/Award Number: MRG6080001; Newton Fund

Abstract

Objective: To delineate orodontal features, dental mineral density, genetic aetiology and cellular characteristics associated with amelogenesis imperfecta (AI).

Materials and Methods: Three affected patients in a family were recruited. Whole-exome sequencing was used to identify mutations confirmed by Sanger sequencing. The proband's teeth were subjected for mineral density analysis by microcomputerised tomography and characterisation of periodontal ligament cells (PDLs).

Results: The patients presented yellow-brown, pitted and irregular enamel. A novel nonsense mutation, c.1261G>T, p.E421*, in exon 5 of the *FAM83H* was identified. The mineral density of the enamel was significantly decreased in the proband. The patient's PDLs (*FAM83H* cells) exhibited reduced ability of cell proliferation and colony-forming unit compared with controls. The formation of stress fibres was remarkably present. Upon cultured in osteogenic induction medium, *FAM83H* cells, at day 7 compared to day 3, had a significant reduction of *BSP*, *COL1* and *OCN* mRNA expression and no significant change in *RUNX2*. The upregulation of *ALP* mRNA levels and mineral deposition were comparable between *FAM83H* and control cells.

Conclusions: We identified the novel mutation in *FAM83H* associated with autosomal dominant hypocalcified AI. The *FAM83H* cells showed reduced cell proliferation and expression of osteogenic markers, suggesting altered PDLs in *FAM83H*-associated AI.

KEYWORDS

calcification, enamel, mineralisation, periodontium, proliferation, stress fibre

1 | INTRODUCTION

Amelogenesis imperfecta (AI) is a genetic condition showing enamel abnormalities in both primary and permanent teeth (Smith et al., 2017). AI exhibits a prevalence as high as one in 700 in some populations (Smith et al., 2017). Tooth discolouration and changes in enamel appearance are common observations (Gadhia, McDonald, Arkutu, & Malik, 2012). Clinical characteristics can be classified into hypoplastic, hypocalcified and hypomatured. Each type is contributed

by different mechanisms. Hypoplastic AI is caused by the failure at secretory stage during enamel formation, while hypocalcified AI is caused by inadequate calcium ion transportation (Smith et al., 2017). Defection in enamel matrix protein removal results in the remaining of protein in mature enamel, causing hypomaturational type of AI (Smith et al., 2017).

Mutations in several genes have been identified to cause AI including *AMELX*, *MMP20*, *ENAM*, *FAM83H*, *WDR72*, *KLK4*, *COL17A1* and *C4orf26*, which contribute to different clinical phenotypes

(Prasad, Laouina, El Alloussi, Dollfus, & Bloch-Zupan, 2016; Wright et al., 2011). Among these genes, mutations in family with sequence similarity 83, member H or *FAM83H* (OMIM *611927) contribute to the majority of autosomal dominant cases and associated with hypocalcified type characterised by enamel showing normal thickness but decreased mineral content (Wright et al., 2011). The reported mutations were localised in the exon 5 of *FAM83H* that truncate the protein and restrict it in the nucleus (Lee et al., 2011; Song, Wang, Zhang, Yang, & Bian, 2012).

FAM83H is expressed by several cell types including ameloblasts, odontoblasts and alveolar bone (Kuga, Sasaki, et al., 2016). It encodes an intracellular protein believed to be associated with keratin cytoskeleton and desmosome (Kuga, Sasaki, et al., 2016). However, the characteristics of cells derived from the patients with *FAM83H* mutations have never been reported. This study identified a novel nonsense mutation in *FAM83H* and characterised phenotypes, dental mineral density and periodontal ligament cells (PDLs) derived from the patient with AI.

2 | MATERIALS AND METHODS

2.1 | Subjects

A Thai family with isolated AI was recruited. The proband, her brother, sister and parents were examined. The study was exempted by Institutional Review Board (IRB No. 163/61, 10 April 2018), Faculty of Medicine, Chulalongkorn University, and followed the Declaration of Helsinki (version 2002) and the additional requirements. Informed written consents were obtained from all participants.

2.2 | DNA isolation and exome sequencing

The proband, her brother and her parents participated in the genetic studies. The peripheral blood leucocytes were subjected to extraction of genomic DNA. The DNA sample was prepared according to previous publications (Porntaveetus, Srichomthong, Suphapeetiporn, & Shotelersuk, 2017). Sequencing was performed at Macrogen, Inc. (Seoul, Korea). GATK with HaplotypeCaller was used for variant calling. SnpEff and annotation databases including dbpSNP142, ClinVar, ESP and 1,000 Genomes were used to annotate SNVs and indels. The variant was considered novel when it was not found in Exome Aggregation Consortium database (exac.broadinstitute.org), Human Gene Mutation database (www.hgmd.cf.ac.uk/ac/index.php) and our in-house database of 1,200 unrelated Thai exomes.

2.3 | Sanger sequencing

Sanger sequencing was employed to confirm the variant. The DNA treated with ExoSAP-IT (USP Corporation, Cleveland, OH, USA) was sent to Macrogen for sequencing. The data were analysed by Sequencher (v.5.0; Gene Codes Corporation, Ann Arbor, MI, USA). Supporting information Table S1 demonstrated the primer sequences.

2.4 | Mineral density

The unerupted upper left third molar that was removed according to the orthodontic treatment plan was analysed by microcomputerised tomographic machine (μ CT35; Scanco Medical, Switzerland). Thirty areas in the enamel and dentine were selected to determine the mineral density, compared with the same areas of the tooth from healthy individual.

2.5 | Cell isolation

The periodontal ligament cells (PDLs) were isolated from the proband's upper right second premolar which was extracted according to the orthodontic treatment plan. Similar passage of cells from healthy individuals was used as the controls. Cell isolation protocol was performed according to previous publications (Nowwarote, Osathanon, Jitjaturunt, Manopattanasoontorn, & Pavasant, 2013; Osathanon et al., 2015). Teeth were rinsed with phosphate-buffered saline, and periodontal tissues at the middle third of the root length were gently scraped. Cell explant technique was performed by placing periodontal tissues on 35-mm culture dishes and maintained in Dulbecco's modified Eagle medium (DMEM; Gibco, USA) supplemented with 10% foetal bovine serum, 100 U/ml penicillin, 2 mM L-glutamine, 250 ng/ml amphotericin B and 100 μ g/ml streptomycin. Cells were incubated in 100% humidity with 5% carbon dioxide at 37°C. Culture medium was changed every 2 days. After reaching confluence, the cells were subcultured at 1:3 ratios. The PDLs at passage 5 were used.

2.6 | Cell proliferation assay

Cell proliferation was determined using 3-(4,5-dimethylthiazol-2-yl)-2,5-diphenyltetrazolium bromide (MTT) assay (Manokawinchoke et al., 2017; Sukarawan, Nowwarote, Kerdpon, Pavasant, & Osathanon, 2014). A total of 12,500 cells per well were seeded and maintained in growth medium. They were incubated with MTT solution (1 mg/ml) for 10 min at days 1, 3 and 7. The formazan crystals were subsequently dissolved by 1 ml mixed solution of glycine buffer and dimethylsulfoxide. The optical density was determined at 570 nm.

2.7 | Colony-forming unit assay

Cells were seeded at 500 cells per dish, maintained in growth medium for 14 days, fixed with 4% formalin and stained with methylene blue.

2.8 | Immunofluorescence staining

Cells fixed in 3% glutaraldehyde (Fluka Analytical, USA) for 10 min were permeabilised with 0.1% Triton[®] X-100 (Sigma-Aldrich, USA) for 1 min. They were then stained with 1:100 rhodamine-phalloidin (Invitrogen, USA) in 10% horse serum for 15 min at room

temperature. DAPI was used for nuclei counterstaining. The fluorescence was evaluated by fluorescence microscope (ZEISS, Germany).

2.9 | Scanning electron microscopic (SEM) analysis

Cells fixed with 3% glutaraldehyde for 30 min were dehydrated with a graded series of ethanol. These were followed by the critical point dried process, sputter-coated with carbon and analysed by SEM (Quanta 250, FEI, Hillsboro, OR, USA).

2.10 | Osteogenic differentiation

Cells were seeded (25,000 cells/well) in 24-well plate and left to attach for 24 hr. The culture medium was changed to osteogenic induction medium supplemented with Dex (100 nM), β -glycerophosphate (10 mM) and ascorbic acid (50 μ g/ml). Cells isolated from each donor, including proband, were maintained in osteogenic induction medium in quadruplicate.

2.11 | Mineralisation assay

After rinsing with deionised water, cells were fixed with cold methanol for 10 min. They were incubated for 3 min with 1% alizarin red S solution.

2.12 | Polymerase chain reaction

Total RNA was extracted by RiboEx solution (GeneAll, Korea). One microgram of total RNA was converted to cDNA (Promega, Madison, WI, USA). Real-time polymerase chain reaction was performed using FastStart[®] Essential DNA Green Master (Roche, USA) and MiniOpticon system (Bio-Rad). A melting curve analysis was used to determine the product specificity. Expression value was normalised to 18S (Supporting information Table S1).

2.13 | Statistical analyses

The experiments were performed in quadruplicate. Two-group comparison was determined using Mann-Whitney *U* test (Prism7; GraphPad Software, CA, USA). The *p* value <0.05 was considered statistically significant.

3 | RESULTS

3.1 | Phenotypic characterisation

The proband is a 21-year-old Thai woman. She first presented at 11 years of age for dental treatment due to discoloured teeth. Her teeth were rough, pigmented and yellow-brown in colour, covered with plaque and calculus and had multiple dental cavities. The gingiva was generally inflamed. Posteruptive breakdown was observed soon after tooth eruption. The patient had received multiple dental restorations for the past 10 years. The proband, her siblings and her

parents were recruited for genetic studies. At 17 years of age, the proband's teeth showed generalised enamel porosity and vertical grooves on the labial/buccal surfaces. The enamel was severely deteriorated exposing the dentine. The height and width of tooth crowns were decreased demonstrating the loss of proximal and interocclusal spaces. The focal spots of normal-looking enamel were presented at the cusp tips and cervical areas of the crowns (Figure 1a-d). Dental radiographs at 17 years of age showed that the erupted teeth had rough and thin enamel with reduced radiopacity, while unerupted third molars showed thick layer of enamel (Figure 1e). Her lower left second premolar spontaneously developed apical infection causing perimandibular space abscess. Incision and drainage and endodontic treatment were employed. At 19 years of age, the radiographs exhibited progressive deterioration of enamel, loss of proximal contact and more crowded teeth (Figure 1f-h). The levels of Mutans streptococci (5.9×10^5 CFU/ml) and Lactobacilli (7.5×10^5 CFU/ml) in her oral cavity were high. The final treatment plan included orthodontic treatment with miniscrew, crown lengthening, osteoplasty and full coverage crowns on all teeth. The upper right first premolar and unerupted third molars were extracted. Orthodontic analyses showed class I malocclusion (Figure 1i). Micro-CT analyses demonstrated the proband's upper left third molar had the reduction in the opacity and mineral density of the enamel (1,332.36 mg HA/cm²), compared to the control (2,011.38 mg HA/cm²). The mineral density of the proband's dentine (1,143.17 mg HA/cm²) was comparable to the control (1,176.65 mg HA/cm²) (Figure 1j,k). Her older brother exhibited similar dental characteristics to the proband (Figure 1l-n). Her father had only two teeth with prosthetic crowns. Besides having abnormal teeth, the proband, her brother and her father were healthy.

3.2 | Genetic investigations

Mutation analysis was performed by whole-exome sequencing. The total yield of 5,917,051,468 bp was achieved. The capture efficiency was 97.3% (>10 \times). The mean read depth was 68.4 \times at target regions. The mutation was screened in ExAC, HGMD and in-house databases. Sanger sequencing of the candidate variants was performed. It was found that the proband, her brother and her father harboured a novel heterozygous substitution (c.1261G>T) in exon 5 of *FAM83H* (NM_198488.3), resulting in a nonsense mutation (p.E421*) at codon 421 (Figure 2a-c).

3.3 | Characterisation of PDLCs

The PDLCs were isolated from the proband (*FAM83H* cells) and healthy donors. The *FAM83H* cells exhibited similar morphology to those of the control donor cells (Figure 3a). According to the proliferation assay, the cell number of *FAM83H* cells, at day 7, was increased compared to those at day 1, suggesting proliferation ability of the cells (Figure 3b). However, the cell number of *FAM83H* was significantly less than that of the controls at day 3 and day 7. Correspondingly, *FAM83H* cells exhibited lower colony-forming unit



FIGURE 1 Phenotypic characterisation of the family. (a–d) Maxillary, mandibular, right and anterior views of oral photographs of the proband showed yellow-brown, pitted, grooved and irregular enamel of the teeth. The teeth were deteriorated and crowding. The cervical enamel and tips of tooth cusps were less affected. (e) Panoramic radiograph of the proband at 17 years of age demonstrated irregular enamel with reduced radiopacity. The lower right second premolar developed periapical lesion. (f–h) The proband at age 19 years revealed progressive destruction of the enamel, loss of proximal contact and several dental cavities. (i) Lateral cephalometric radiograph showed class I malocclusion. (j) Microcomputerised tomography of the proband's third molar showed loss of enamel with decreased radiopacity compared with the control. (l–n) Radiographs of the proband's brother exhibited similar characteristics to the proband [Colour figure can be viewed at wileyonlinelibrary.com]

compared with the control cells (Figure 3c). The expression of genes related to proliferation and apoptosis was determined at day 3. The level of a proliferative marker *MKI67* was reduced in *FAM83H* cells compared with the control; however, there was no marked difference in the expression of apoptosis-related genes, *BAD*, *BCL2* and *BAX* (Supporting information Figure S1).

Cell attachment and spreading properties were evaluated using phalloidin immunofluorescence staining and SEM. At 30 min after seeding, cells in all groups were able to attach on the tissue culture plate (Figure 4). F-actin filaments were predominantly observed at

the peripheral edge of the cells. At 2 hr, cell spreading was noted in all groups. However, stress fibres were more organised in the cytoplasm of *FAM83H* cells with focal accumulation of F-actin at the edge of cells. In the control cells, F-actin filaments were still mainly noted at the peripheral edge of the cells. At 6 and 24 hr, cells in all groups were able to spread and present stress fibre formation, but *FAM83H* cells demonstrated remarkable organised stress fibres compared with the control cells.

Representative SEM images were presented in Figure 5. Correspondingly, *FAM83H* cells formed extended

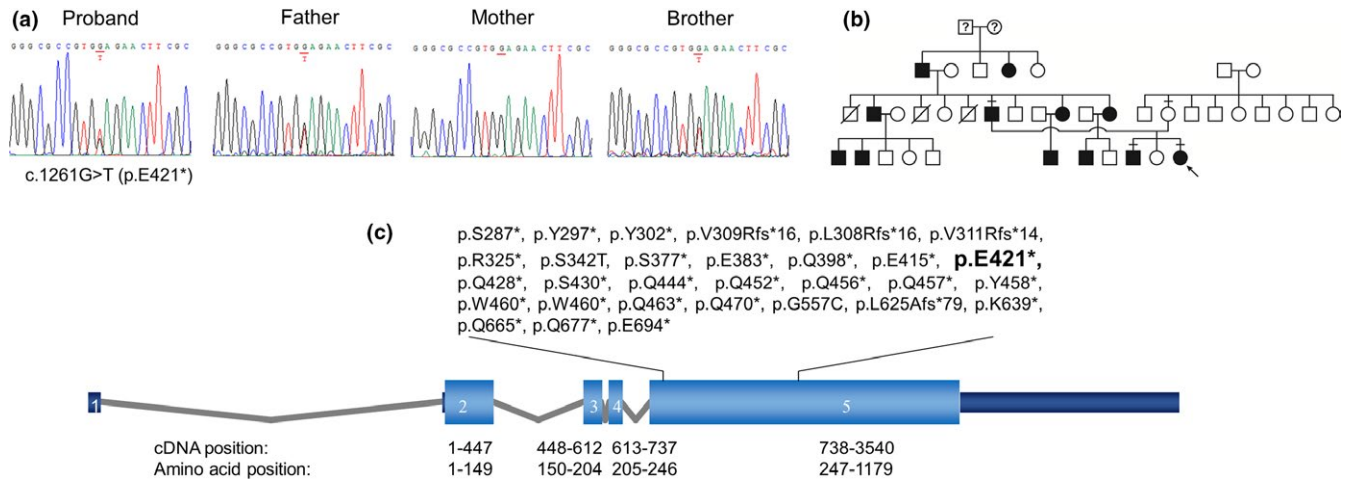


FIGURE 2 Genetic analyses and pedigree of the family. (a) Electropherograms demonstrated a novel heterozygous nonsense mutation, c.1261G>T, p.E421*, in exon 5 of the *FAM83H* in the proband, her brother and her father. The mutation was not observed in his unaffected mother. (b) A pedigree of the proband's family. The blackened symbol represented the clinically affected individual. An arrow indicated the proband. The horizontal lines above individual's symbols represented the persons recruited for genetic studies. (c) Diagram represented the *FAM83H* gene (NM_198488.3). Reported mutations were indicated above the diagram (*FAM83H*, NP_940890.3) [Colour figure can be viewed at wileyonlinelibrary.com]

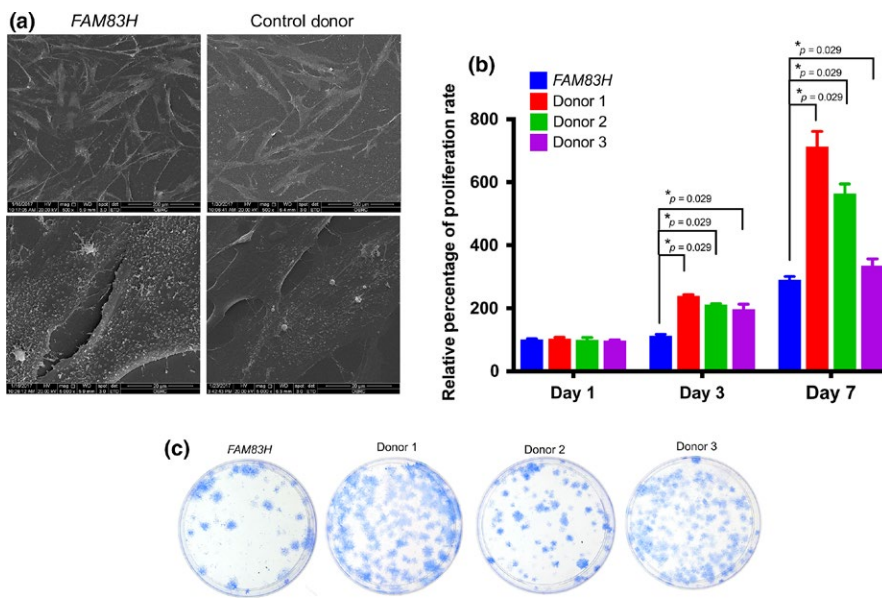


FIGURE 3 Cell morphology and proliferation of PDLCs. (a) Scanning electron microscope demonstrated that *FAM83H* cells had similar morphology to the controls. (b) *FAM83H* cells exhibited lower cell number compared to the control cells at day 3 and day 7. Data were presented as mean \pm standard deviation. (c) Colony-forming units of *FAM83H* cells were lower than those of controls. Bars indicated the statistically significant difference [Colour figure can be viewed at wileyonlinelibrary.com]

circumferential lamellipodia at 30 min and 2 hr, and most cells were completely flat at 6 hr after seeding. On the contrary, the control cells exhibited the domelike morphology with minimally extended lamellipodia. No obvious difference in cell spreading and morphology was noted at 6 and 24 hr.

The expression of osteogenic marker gene was examined at days 3 and 7 after incubation in osteogenic medium. The significant increase of *RUNX2* mRNA expression was observed in the controls, but not in *FAM83H* cells (Figure 6a). The *ALP* mRNA expression was upregulated in all groups at day 7 compared with day 3 at which the lowest fold change was detected in *FAM83H* cells (Figure 6b). Further, *FAM83H* cells exhibited significant reduction of *BSP*, *COL1* and *OCN* mRNA levels at day 7 compared with day 3 (Figure 6c-e).

An in vitro mineralisation was examined in the cells maintained in osteogenic medium for 14 days (Figure 6f). Cells in growth medium were employed as the control. Results demonstrated that an in vitro mineralisation ability was not markedly different between the control and *FAM83H* cells.

4 | DISCUSSION

The present study identified the novel nonsense mutation, c.1261G>T, p.E421*, in the exon 5 of *FAM83H* in a Thai family. The rough and yellow-brown enamel with focal areas of normal enamel appearance presenting at the tooth cusps and cervical areas was consistent with the typical features of autosomal dominant

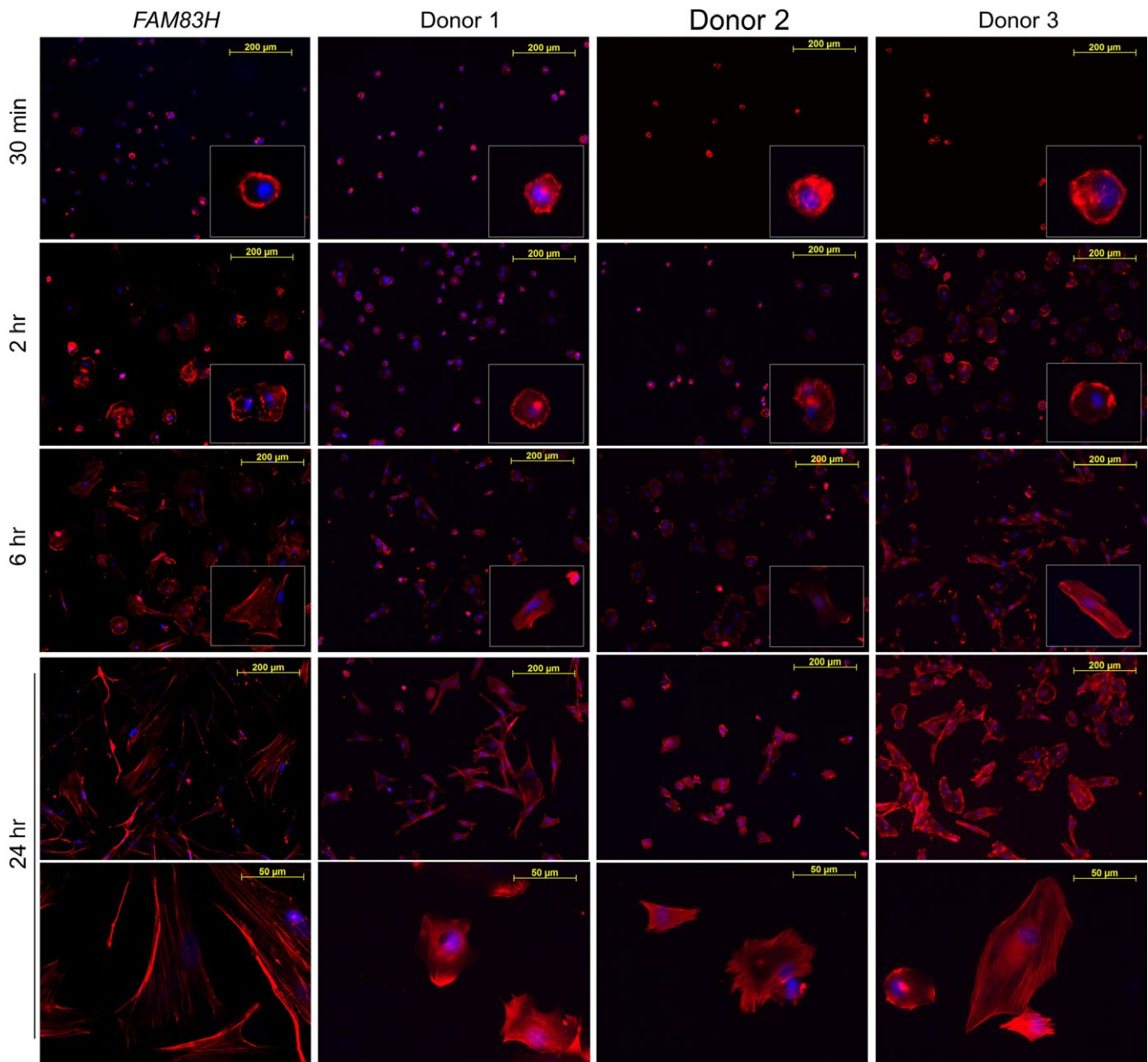


FIGURE 4 Cell attachment and spreading. Cells seeded on tissue culture plate for 30 min, 2, 6 and 24 hr showed F-actin orientation during cell attachment and spreading. F-actin was stained with rhodamine–phalloidin. *FAM83H* cells exhibited more organised stress fibres compared to the controls at 2, 6 and 24 hr [Colour figure can be viewed at wileyonlinelibrary.com]

hypocalcified AI (ADHCAI). Radiographically, the enamel of erupted teeth was generally thin and reduced in density. Mineral density analyses revealed that patient's enamel had significantly reduced mineral density compared with the control, suggesting the defects in calcification process during amelogenesis. These phenotypes and genotypes confirm the diagnosis of ADHCAI in this family.

Diverse dental and skeletal phenotypes have been observed in various populations with *FAM83H* mutations (Wright et al., 2009). It was reported that the patients having short *FAM83H* protein of fewer 677 amino acids exhibited generalised ADHCAI, while mutations producing at least 694 amino acids had limited defects only at the cervical enamel (Wright et al., 2009). This is consistent with

our patients, p.E421*, who showed generalised AI. Besides enamel defects, class III malocclusion and anterior open bite were the most commonly reported features in AI (Poulsen et al., 2008; Wright et al., 2009). The proband and her brother, however, did not have skeletal malocclusion.

Thirty mutations (24 nonsense, four frameshift and two missense) in *FAM83H*, including our novel mutation, have been associated with ADHCAI in various populations (Supporting information Table S2). All but two were truncating mutations locating within the last exon, exon 5, of *FAM83H*. These truncated transcripts are not generally subject to nonsense mediated decay (Nagy & Maquat, 1998). Overexpression of *FAM83H* in mice and *Fam83h* null mice did

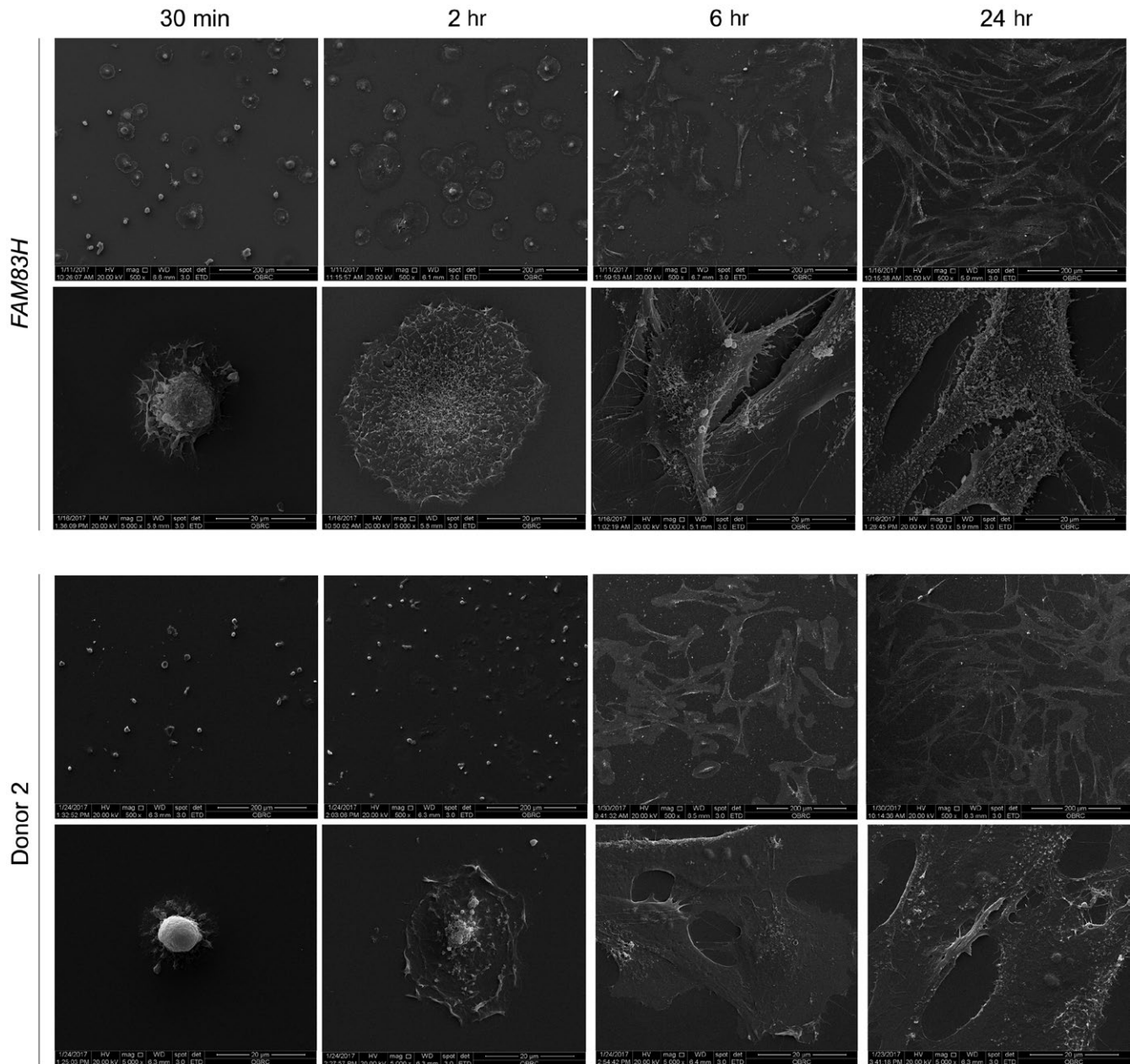


FIGURE 5 Actin projection. SEM micrographs revealed that *FAM83H* cells formed extended circumferential lamellipodia around the cells at 30 min and 2 hr, while the control cells exhibited minimal lamellipodia. No obvious difference in cell spreading and morphology was noted at 6 and 24 hr

not show distinct enamel phenotypes compared to the wild-type mice (Kweon et al., 2013; Wang et al., 2016). These suggest that the pathogenic mechanisms of *FAM83H* mutations causing ADHCAI are likely caused by gain of function or dominant negative effect of mutated *FAM83H* rather than loss of function or haploinsufficiency.

Fam83h was expressed in the murine presecretory and secretory ameloblasts, odontoblasts and surrounding periodontium (Lee et al., 2009). Functional studies showed that it was localised on keratin filaments and truncated *FAM83H* disturbed the organisation of the keratin cytoskeleton and desmosomes in human ameloblastoma cells (Kuga, Kume, et al., 2016; Wang et al., 2016). The mutant, instead of normal cytoplasmic location, was shown to concentrate

in the nucleus (Lee et al., 2011). These studies have proposed the pathophysiology of *FAM83H*; however, its role in actin filament and calcification process has not been revealed. We therefore determined the cytoskeleton formation in our *FAM83H* mutant cells. They showed the formation of stress fibres at early time point. At 2 hr, stress fibre organisation in cytoplasm and focal accumulation at the membrane edge were demonstrated in *FAM83H* mutant cells, while F-actin filaments were still mainly noted at the peripheral edge of the control cells. Advanced stage of cell spreading was seen in *FAM83H* mutant cells, compared with the controls. These suggest that *FAM83H* mutant cells were able to form actin stress fibre. Several studies demonstrated the positive correlation between stress fibre

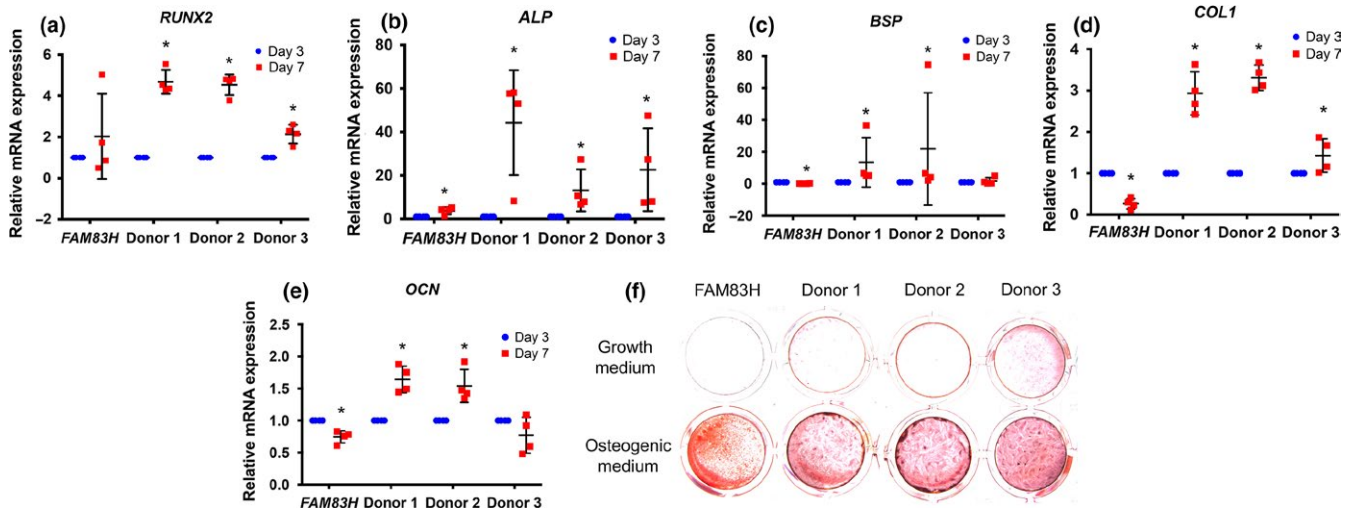


FIGURE 6 Expression of osteogenic markers and mineral deposition. (a) Real-time quantitative polymerase chain reaction showed the significant increase of *RUNX2* mRNA expression in the control cells at day 7 compared with day 3, but no significant difference was observed in *FAM83H* cells. (b) The *ALP* mRNA expression was upregulated in all groups at day 7 compared with day 3. The lowest fold change was observed in *FAM83H* cells. (c–e) *FAM83H* cells exhibited significant reduction of *BSP*, *COL1* and *OCN* mRNA levels at day 7 compared with day 3. (f) An in vitro mineralisation ability was not markedly different between the control and *FAM83H* cells. Asterisks represented the statistically significant difference compared to day 3. The middle line represented mean values. The top and bottom bars indicated standard deviation values [Colour figure can be viewed at wileyonlinelibrary.com]

formation and cell proliferation. However, it was revealed that mTOR kinase domain inhibitors could inhibit murine fibroblast cell proliferation without influencing on actin stress fibres (Feldman et al., 2009). Moreover, thalidomide-treated endothelial cells showed promoted actin polymerisation but attenuated cell migration and proliferation (Tamilarasan et al., 2006). Hence, these imply that the actin stress fibre formation in *FAM83H* mutant cells might not directly associate with its proliferation and colony-forming abilities, or the effect of *FAM83H* mutation might be specific for particular types of cytoskeleton protein and cells.

The mineralisation and osteogenic gene expression are related processes but diversely controlled by several regulatory mechanisms. *FAM83H* has been shown to inhibit mineralisation and lower the expression of the mineralisation factors *Runx2*, *Alp* and *Ocn* (Yang et al., 2018). We observed that *FAM83H* mutant cells had impaired expression of osteogenic marker genes (*BSP*, *COL1* and *OCN*) at day 7 compared to day 3. The *BSP* was strongly expressed in bone and participates in bone formation. The calvaria cells from *Bsp*^{-/-} mice exhibited the reduction of cell proliferation and colony-forming unit (Bouet et al., 2015). In the present study, we observed the significant decrease of *BSP* levels in *FAM83H* mutant cells which also showed slow rate of proliferation. Correspondingly, the cells from healthy donor that exhibited low *BSP* expression had inferior cell proliferation ability. The *OCN* was shown to stimulate osteoblast differentiation and osteocyte maturation participating in bone matrix mineralisation (Shao et al., 2015). The *FAM83H* mutant cells showed reduced *OCN* expression while maintained mineralisation ability. Several reports demonstrated that the *OCN* expression was not directly associated with in vitro mineralisation due to alternative regulations of osteogenic differentiation. In this regard,

Jagged1 markedly upregulated mineralisation in PDLCs without the increase of *OCN* level (Osathanon et al., 2013). Further, knocked-down *Twist* gene in PDLCs enhanced osteogenic differentiation and mRNA expression of *ALP*, *OPN* and *BSP*, but not *OCN* (Komaki et al., 2007).

The *ALP* has been shown to cleave extracellular pyrophosphate, an inhibitor of mineralisation, resulting in the accumulation of extracellular inorganic phosphate and the precipitation and growth of mineral crystals. We observed the upregulation of *ALP* mRNA level at day 7 compared with day 3 in all groups of cells, suggesting that their abilities to generate inorganic phosphate and deposit mineral crystals were still intact. A number of genes including *ALP*, *ENPP1*, *ANKH* and *PIT1* were shown to control phosphate metabolism and extracellular phosphate/pyrophosphate ratio that influences mineral deposition. These illustrate the complex interactions among osteogenic-related genes during mineralisation. It is therefore possible that mineralisation process still occurs although the expression levels of certain osteogenic marker genes are altered. In addition, the PDLCs isolated from the patient are primary cells containing heterogeneous population that could result in wide-variation data.

The indirect association of *Fam83h* on mineralisation was formerly reported in murine ameloblast cell line (Jia, Yang, Yang, Wang, & Song, 2016). They showed that fluoride treatment resulted in decreased *ALP* enzymatic activity in ameloblasts, and correspondingly, fluoride inhibited *Fam83h* expression at mRNA and protein levels (Jia et al., 2016). It was suggested that fluoride-attenuated *Fam83h* expression might be related to the reduction of mineralisation via the decrease of *ALP* enzymatic activity. These observations contradicted to our study which can be explained by

the following aspects. First, the types and species of cells were used. Second, the influence of *Fam83h* on ALP enzymatic activity was indirectly implied in mouse ameloblasts according to the decreased *Fam83h* expression and ALP activity after fluoride treatment (Jia et al., 2016), whereas the present study investigated the mineralisation ability of *FAM83H* human PDLCs. However, further functional study should be performed to identify the role of *FAM83H* mutation on osteogenic differentiation and mineralisation process.

The multidisciplinary treatment planning for the patient included orthodontic treatment with miniscrew, crown lengthening, osteoplasty and full coverage crowns on all teeth aimed at functional occlusion and improved aesthetics and psychosocial condition of the patient. An ideal occlusion might not always be the treatment goal for AI patients due to complex craniofacial and dental abnormalities (Arkutu, Gadhia, McDonald, Malik, & Currie, 2012). Orthodontic treatments in AI patients showed a successful outcome with satisfied post-treatment stability (Bechor, Finkelstein, Shapira, & Shpack, 2014; Yilmaz, Oz, & Yilmaz, 2014). Remodelling of alveolar bone and periodontal ligaments is associated with orthodontic tooth movement. Our study observed that *FAM83H* mutant PDLCs showed the reduction of proliferation, colony forming and osteogenic gene expression while maintained mineral deposition. These altered cellular characteristics could affect periodontal homeostasis and dynamic alterations upon applying orthodontic forces. Close monitoring of periodontal status should therefore be employed for AI patient. The cellular effects of orthodontic forces on the periodontium including periodontal ligaments and alveolar bone of AI patient should be further studied.

To conclude, we have identified the novel nonsense mutation, c.1261G>T, p.E421*, in the *FAM83H* gene in a Thai family. The phenotypes and genotypes confirm the diagnosis of the ADHCAI. Our study is the first to reveal the characteristics of cells isolated from the *FAM83H* patient which shows the reduction in proliferation and expression of osteogenic markers. This study expands mutation spectrum of *FAM83H* and demonstrates its cellular characteristics in calcification processes, contributing to the better understanding of ADHCAI.

ACKNOWLEDGEMENTS

The study was supported by the Thailand Research Fund (TRF) (DPG6180001) and Office of Higher Education Commission (OHEC), Thailand (MRG6080001), the Newton Fund and the Chulalongkorn Academic Advancement Into Its 2nd Century Project. Nunthawan Nowwarote is supported by the Rachadapisek Sompote Fund for Postdoctoral Fellowship, Chulalongkorn University. We thank Thimaporn BuchakorSemporn for carrying out dental treatment for the patient and Lawan Boonprakong and Anucharte Srijunbarl for handling the SEM.

CONFLICTS OF INTERESTS

The author declared no conflict of interests.

AUTHOR CONTRIBUTIONS

N. Nowwarote contributed to designing the study, analysing the data and revising the manuscript; T Theerapanon, P Pavasant and V Shotelersuk contributed to obtaining and analysing the data and revising the manuscript; T Osathanon contributed to planning the study, analysing the data and revising the manuscript. T. Pornraveetus contributed to planning the study, analysing the data, drafting and revising the manuscript.

ORCID

Prasit Pavasant  <http://orcid.org/0000-0002-8909-5928>

Thantrira Pornraveetus  <http://orcid.org/0000-0003-0145-9801>

REFERENCES

- Arkutu, N., Gadhia, K., McDonald, S., Malik, K., & Currie, L. (2012). Amelogenesis imperfecta: The orthodontic perspective. *British Dental Journal*, 212(10), 485–489. <https://doi.org/10.1038/sj.bdj.2012.415>
- Bechor, N., Finkelstein, T., Shapira, Y., & Shpack, N. (2014). Conservative orthodontic treatment for skeletal open bite associated with amelogenesis imperfecta. *Journal of Dentistry for Children (Chic)*, 81(2), 96–102.
- Bouet, G., Boulefour, W., Juignet, L., Linossier, M.-T., Thomas, M., Vanden-Bossche, A., & ... Malaval, L. (2015). The impairment of osteogenesis in bone sialoprotein (BSP) knockout calvaria cell cultures is cell density dependent. *PLoS ONE*, 10(2), e0117402. <https://doi.org/10.1371/journal.pone.0117402>
- Feldman, M. E., Apsel, B., Uotila, A., Loewith, R., Knight, Z. A., Ruggero, D., & Shokat, K. M. (2009). Active-site inhibitors of mTOR target rapamycin-resistant outputs of mTORC1 and mTORC2. *PLOS Biology*, 7(2), e1000038. <https://doi.org/10.1371/journal.pbio.1000038>
- Gadhia, K., McDonald, S., Arkutu, N., & Malik, K. (2012). Amelogenesis imperfecta: An introduction. *British Dental Journal*, 212(8), 377–379. <https://doi.org/10.1038/sj.bdj.2012.314>
- Jia, J., Yang, F., Yang, M., Wang, C., & Song, Y. (2016). P38/JNK signaling pathway mediates the fluoride-induced down-regulation of *Fam83h*. *Biochemical and Biophysical Research Communications*, 471(3), 386–390. <https://doi.org/10.1016/j.bbrc.2016.02.027>
- Komaki, M., Karakida, T., Abe, M., Oida, S., Mimori, K., Iwasaki, K., & ... Ishikawa, I. (2007). Twist negatively regulates osteoblastic differentiation in human periodontal ligament cells. *Journal of Cellular Biochemistry*, 100(2), 303–314. <https://doi.org/10.1002/jcb.21038>
- Kuga, T., Kume, H., Adachi, J., Kawasaki, N., Shimizu, M., Hoshino, I., & ... Tomonaga, T. (2016). Casein kinase 1 is recruited to nuclear speckles by *FAM83H* and *SON*. *Scientific Reports*, 6, 34472. <https://doi.org/10.1038/srep34472>
- Kuga, T., Sasaki, M., Mikami, T., Miake, Y., Adachi, J., Shimizu, M., & ... Nakayama, Y. (2016). *FAM83H* and casein kinase I regulate the organization of the keratin cytoskeleton and formation of desmosomes. *Scientific Reports*, 6, 26557. <https://doi.org/10.1038/srep26557>
- Kweon, Y. S., Lee, K. E., Ko, J., Hu, J. C., Simmer, J. P., & Kim, J. W. (2013). Effects of *Fam83h* overexpression on enamel and dentine formation. *Archives of Oral Biology*, 58(9), 1148–1154. <https://doi.org/10.1016/j.archoralbio.2013.03.001>
- Lee, S. K., Lee, K. E., Jeong, T. S., Hwang, Y. H., Kim, S., Hu, J. C., & ... Kim, J. W. (2011). *FAM83H* mutations cause ADHCAI and alter intracellular protein localization. *Journal of Dental Research*, 90(3), 377–381. <https://doi.org/10.1177/0022034510389177>

- Lee, M. J., Lee, S. K., Lee, K. E., Kang, H. Y., Jung, H. S., & Kim, J. W. (2009). Expression patterns of the Fam83h gene during murine tooth development. *Archives of Oral Biology*, 54(9), 846–850. <https://doi.org/10.1016/j.archoralbio.2009.05.009>
- Manokawinchoke, J., Nattasit, P., Thongngam, T., Pavasant, P., Tompkins, K. A., Egusa, H., & Osathanon, T. (2017). Indirect immobilized Jagged1 suppresses cell cycle progression and induces odonto/osteogenic differentiation in human dental pulp cells. *Scientific Reports*, 7(1), 10124. <https://doi.org/10.1038/s41598-017-10638-x>
- Nagy, E., & Maquat, L. E. (1998). A rule for termination-codon position within intron-containing genes: When nonsense affects RNA abundance. *Trends in Biochemical Sciences*, 23(6), 198–199. [https://doi.org/10.1016/S0968-0004\(98\)01208-0](https://doi.org/10.1016/S0968-0004(98)01208-0)
- Nowwarote, N., Osathanon, T., Jitjaturunt, P., Manopattanasoontorn, S., & Pavasant, P. (2013). Asiaticoside induces type I collagen synthesis and osteogenic differentiation in human periodontal ligament cells. *Phytotherapy Research*, 27(3), 457–462. <https://doi.org/10.1002/ptr.4742>
- Osathanon, T., Ritprajak, P., Nowwarote, N., Manokawinchoke, J., Giachelli, C., & Pavasant, P. (2013). Surface-bound orientated Jagged-1 enhances osteogenic differentiation of human periodontal ligament-derived mesenchymal stem cells. *Journal of Biomedical Materials Research Part A*, 101(2), 358–367. <https://doi.org/10.1002/jbm.a.34332>
- Osathanon, T., Vivatbutsiri, P., Sukarawan, W., Sriarj, W., Pavasant, P., & Sooampon, S. (2015). Cobalt chloride supplementation induces stem-cell marker expression and inhibits osteoblastic differentiation in human periodontal ligament cells. *Archives of Oral Biology*, 60(1), 29–36. <https://doi.org/10.1016/j.archoralbio.2014.08.018>
- Porntaveetus, T., Srichomthong, C., Suphapeetiporn, K., & Shotelersuk, V. (2017). Monoallelic FGFR3 and Biallelic ALPL mutations in a Thai girl with hypochondroplasia and hypophosphatasia. *American Journal of Medical Genetics. Part A*, 173(10), 2747–2752. <https://doi.org/10.1002/ajmg.a.38370>
- Poulsen, S., Gjørup, H., Haubek, D., Haukali, G., Hintze, H., Lovschall, H., & Errboe, M. (2008). Amelogenesis imperfecta - a systematic literature review of associated dental and oro-facial abnormalities and their impact on patients. *Acta Odontologica Scandinavica*, 66(4), 193–199. <https://doi.org/10.1080/00016350802192071>
- Prasad, M. K., Laouina, S., El Alloussi, M., Dollfus, H., & Bloch-Zupan, A. (2016). Amelogenesis imperfecta: 1 family, 2 phenotypes, and 2 mutated genes. *Journal of Dental Research*, 95(13), 1457–1463. <https://doi.org/10.1177/0022034516663200>
- Shao, J., Wang, Z., Yang, T., Ying, H., Zhang, Y., & Liu, S. (2015). Bone regulates glucose metabolism as an endocrine organ through osteocalcin. *International Journal of Endocrinology*, 2015, 967673. <https://doi.org/10.1155/2015/967673>
- Smith, C. E. L., Poulter, J. A., Antanaviciute, A., Kirkham, J., Brookes, S. J., Inglehearn, C. F., & Mighell, A. J. (2017). Amelogenesis imperfecta: Genes, proteins, and pathways. *Frontiers in Physiology*, 8, 435. <https://doi.org/10.3389/fphys.2017.00435>
- Song, Y. L., Wang, C. N., Zhang, C. Z., Yang, K., & Bian, Z. (2012). Molecular characterization of amelogenesis imperfecta in Chinese patients. *Cells Tissues Organs*, 196(3), 271–279. <https://doi.org/10.1159/000334210>
- Sukarawan, W., Nowwarote, N., Kerdpon, P., Pavasant, P., & Osathanon, T. (2014). Effect of basic fibroblast growth factor on pluripotent marker expression and colony forming unit capacity of stem cells isolated from human exfoliated deciduous teeth. *Odontology*, 102(2), 160–166. <https://doi.org/10.1007/s10266-013-0124-3>
- Tamilarasan, K., Kolluru, G. K., Rajaram, M., Indhumathy, M., Saranya, R., & Chatterjee, S. (2006). Thalidomide attenuates nitric oxide mediated angiogenesis by blocking migration of endothelial cells. *BMC Cell Biology*, 7(1), 17. <https://doi.org/10.1186/1471-2121-7-17>
- Wang, S. K., Hu, Y., Yang, J., Smith, C. E., Richardson, A. S., Yamakoshi, Y., & ... Simmer, J. P. (2016). Fam83h null mice support a neomorphic mechanism for human ADHCAI. *Molecular Genetics & Genomic Medicine*, 4(1), 46–67. <https://doi.org/10.1002/mgg3.178>
- Wright, J. T., Frazier-Bowers, S., Simmons, D., Alexander, K., Crawford, P., Han, S. T., & ... Hart, T. C. (2009). Phenotypic variation in FAM83H-associated amelogenesis imperfecta. *Journal of Dental Research*, 88(4), 356–360. <https://doi.org/10.1177/0022034509333822>
- Wright, J. T., Torain, M., Long, K., Seow, K., Crawford, P., Aldred, M. J., & ... Hart, T. C. (2011). Amelogenesis imperfecta: Genotype-phenotype studies in 71 families. *Cells Tissues Organs*, 194(2–4), 279–283. <https://doi.org/10.1159/000324339>
- Yang, M., Huang, W., Yang, F., Zhang, T., Wang, C., & Song, Y. (2018). Fam83h mutation inhibits the mineralization in ameloblasts by activating Wnt/ β -catenin signaling pathway. *Biochemical and Biophysical Research Communications*, 501(1), 206–211. <https://doi.org/10.1016/j.bbrc.2018.04.216>
- Yilmaz, B., Oz, U., & Yilmaz, H. G. (2014). Interdisciplinary approach to oral rehabilitation of patient with amelogenesis imperfecta. *New York State Dental Journal*, 80(2), 31–35.

SUPPORTING INFORMATION

Additional supporting information may be found online in the Supporting Information section at the end of the article.

How to cite this article: Nowwarote N, Theerapanon T, Osathanon T, Pavasant P, Porntaveetus T, Shotelersuk V. Amelogenesis imperfecta: A novel FAM83H mutation and characteristics of periodontal ligament cells. *Oral Dis*. 2018;24:1522–1531. <https://doi.org/10.1111/odi.12926>